

**PARIS GAMMA**  
*PARIS Technology Concept Definition*  
TRP ETP 137.A – Phase 1



**GNSS-R MEASUREMENTS FOR OCEAN MESOSCALE  
CIRCULATION MAPPING-AN UPDATE**

Technical Note Extract from the PARIS-GAMMA ESTEC/ESA Study, WP1100  
**ESTEC Technical Officer: M. Martin-Neira**

Produced by

**P.Y. Le Traon and G. Dibarboure (CLS Space Oceanography Division)**  
**Giulio Ruffini, Olivier Germain (Starlab)**  
**A. Thompson, C. Mathew (ASTRIUM)**

Contact: [giulio.ruffini@starlab.es](mailto:giulio.ruffini@starlab.es)

*Created January 28, 2003*  
*Released, Sept 2003*

EUROPEAN SPACE AGENCY REPORT  
CONTRACT REPORT

The work described in this report was done under ESA contract.  
Responsibility for the contents resides in the author or organisation that prepared it.

# CONTENTS

- 1 Introduction ..... 3
- 2 Simulation of the GPS sampling and noise characteristics..... 3
- 3 Methods..... 7
- 4 Results ..... 10
- 5 Formal mapping errors ..... 15
- 6 Conclusions ..... 18
- 7 References ..... 18

## 1 Introduction

In this report, the contribution of GNSS altimetry for the mapping of ocean mesoscale circulation is quantified using the Los Alamos North Atlantic model. It updates a study performed by CLS as part of the ESA Paris-Beta Project (Le Traon et al., 2002). The Los Alamos model is known to represent the mesoscale variability quite well and is very well suited to simulate the contribution of sea level measurements (Le Traon et al., 2001). Model sea level fields are subsampled to simulate the typical space/time sampling of GNSS altimeter systems. A realistic measurement noise is added to these simulated measurements. We then evaluate how these simulated measurements can be used to reconstruct the initial model reference fields depending on the different regions and dynamical regimes. This is achieved using a space/time objective mapping technique that takes into account the GNSS measurement noise characteristics and an a priori information on the space and time scales of ocean signals. Formal sea level mapping errors (see Le Traon and Dibarboure, 1999) are also analyzed as they provide an estimation of mapping errors that depend only on sampling, noise and ocean signal characteristics.

## 2 Simulation of the GPS sampling and noise characteristics

A typical space/time sampling of multibeam GPS altimetry was designed and simulated by Astrium and Starlab. It corresponds to a theoretical 3 second sampling of the GPS + Galileo + Inmarsat reflections that would be received by a LEO satellite in a 500 km polar orbit and a 50° field of view. Given the chosen LEO orbit, this sampling repeats exactly every five days. For this simulation, we have used all measurements available at a given time, that is to say up to 5 measurements from GPS reflections, plus 5 more measurements from Galileo reflections and 2 more measurements from Inmarsat reflections. Figure 1a shows the corresponding sampling over a 5-day period over the whole North Atlantic. Colors correspond to different incident angles. Mission characteristics used were:

- Orbit: 5 day repeat, 500 km altitude.
- WV correction: 5 cm error, 25 km, corresponding to NWP corrections (no WVR)
- Antenna provided by Astrium (27 + dB)
- Dual Frequency for ionospheric correction.
- GPS/Galileo/Inmarsat EIRP (GPS: 28.5 dB, Galileo: 30.4 dB, Inmarsat: 27.9 dB).
- Two-way atmospheric attenuation of -1.2 dB
- Mss corresponding to 0.017, (~6-7 m/s)
- Scene brightness temperature= 100 K
- Loss factor of 1 dB
- Noise Figure of 2 dB
- 1-bit-sampling loss of 2 dB

- SNR\_V one shot of direct signal is 20 linear.
- Orbit error: none
- Clock error: none

The budget for a generic GPS-R altimetric mission can now be carried out, linking all different errors to form the overall altimetric error. Table 2-1 shows the list of parameters assumed for such a mission while Table 2-2 presents the corresponding altimetric error budget. It can be seen that the most important contribution to range error is indeed the reflected signal delay error. Finally, **Figure 2-1** illustrates the altimetric error dependence on elevation angle.

GPS EIRP	29.4 dBW
Receiver gain	27 dB
Receiver altitude	500 km
Receiver Loss Factor	1 dB
Receiver Noise Figure	2 dB
1-bit sampling loss	-2 dB
Atmosphere attenuation	-1.2 dB
Ocean mss	0.017
Scene temperature	170 K
Direct signal one-shot SNR (V)	10
Ionospheric factor	1.06
Tropospheric error	5 cm

Table 2-1 Parameters of a generic GPS-R altimetric mission.

	After one shot	After 1 s	After 3 s
Direct signal SNR (V)	10	370	640
Reflected signal SNR (V)	4.7	170	290
Direct signal delay error	6.6m	18 cm	10 cm
Reflected signal delay error	14 m	39 cm	22 cm
Range error	16 m	44 cm	26 cm
Altimetric error	<b>8 m</b>	<b>22 cm</b>	<b>13 cm</b>

Table 2-2 Altimetric error budget for a specular point at nadir ( $T_i=0.8$  ms).

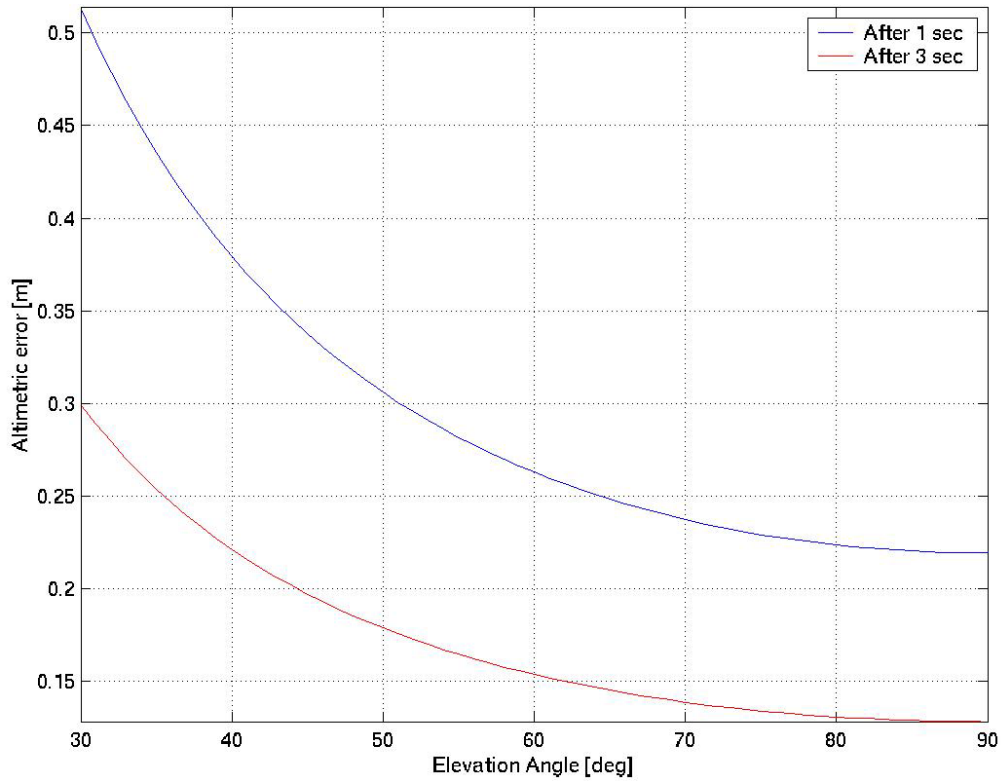
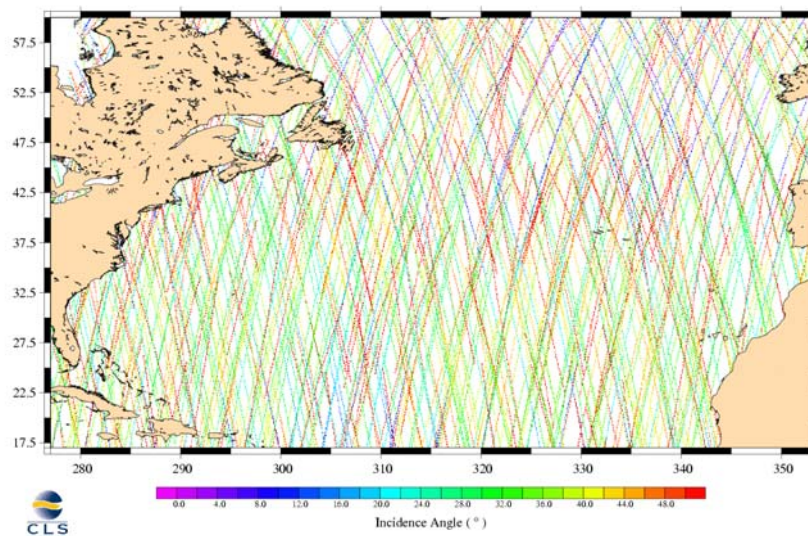


Figure 2-1 Altimetric error vs elevation angle for the generic space mission. Integration time has been set to coherence time for each elevation angle.

The measurement errors  $\epsilon_{GPS}$  for 3 second sampling were computed by Starlab. They are represented on Figure 1b for the 3 constellation sampling, and on Figure 1c, 1d, 1e for each constellation.

**a** 3 Constellations – Incidence Angle



b

3 Constellations – Altimetric Error

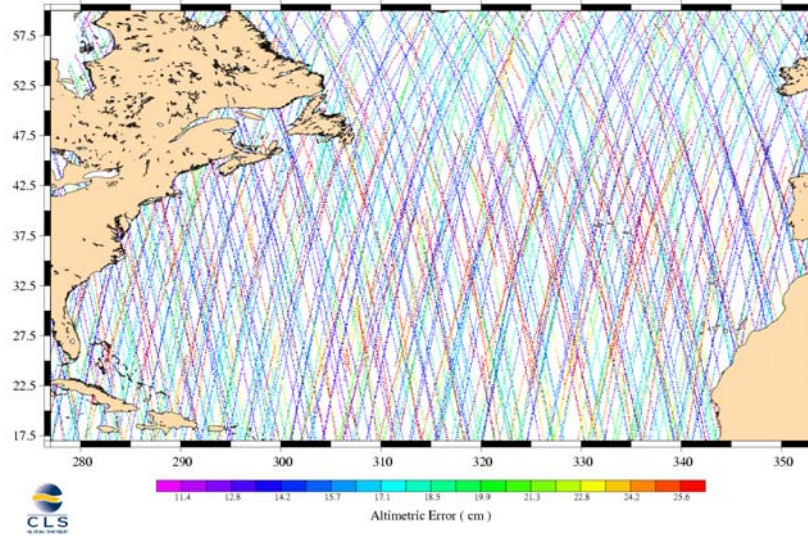
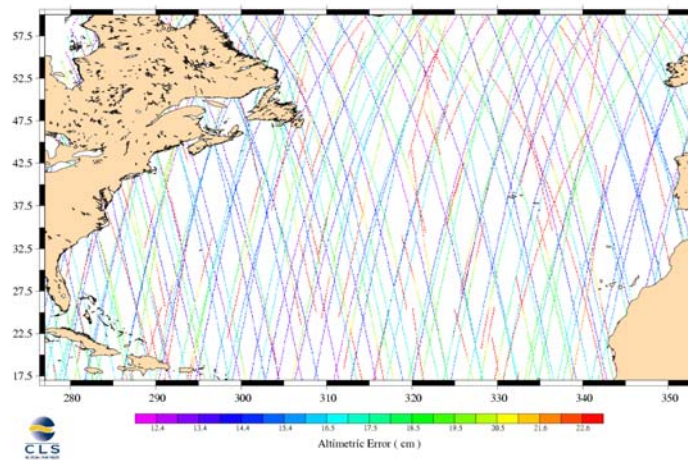


Figure 1a, 1b : 5-day sampling of the North Atlantic from one LEO receiver and the 3 constellation reflections with incidence angle (a) and errors for 3-second averages associated to the local incident angle (b). Units are degree (a) and cm (b).

C

GPS – Altimetric Error



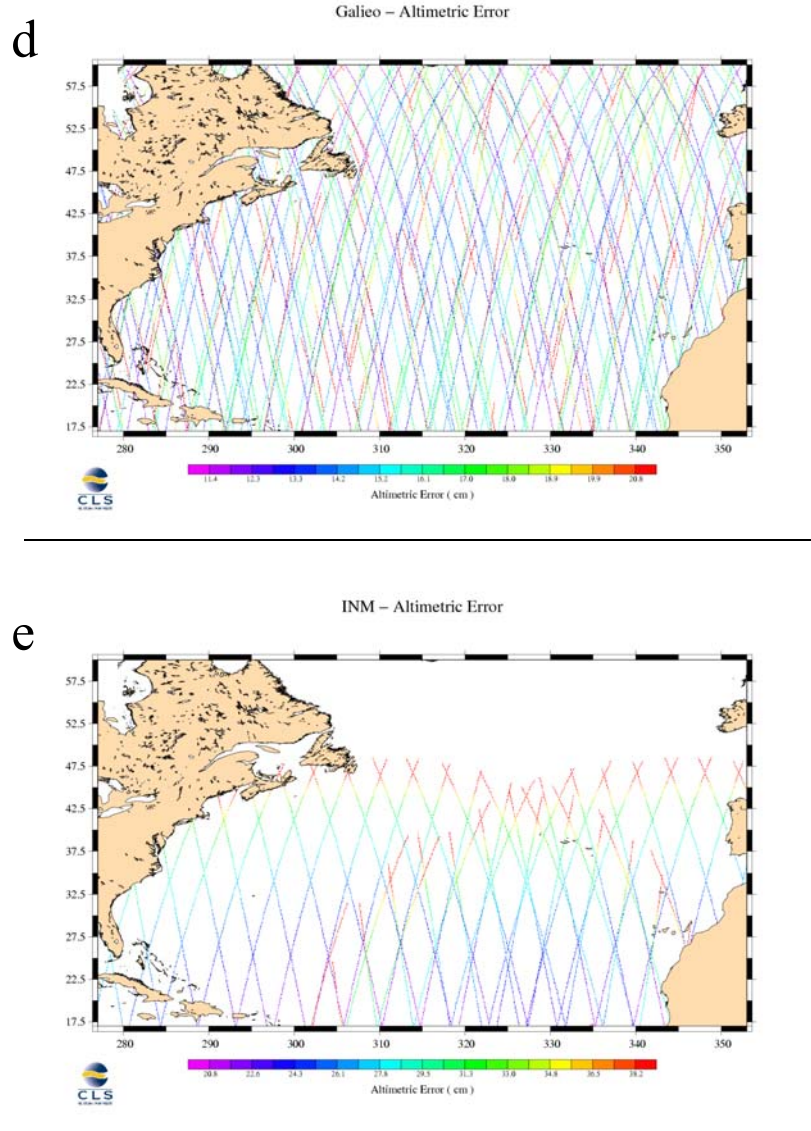


Figure 1c, 1d, 1e : 5-day sampling of the North Atlantic measurements from one LEO with GPS reflections (c) and Galileo reflections (d) and Inmarsat reflections(e).

### 3 Methods

The Los Alamos model (LAM) sea level outputs were first transformed into sea level anomaly data by removing a three-year mean (1993-1995). They were then sub-sampled to obtain simulated GNSS signals along the tracks shown on figure 1. A random noise depending on incident angle (see equation 1) was then added to the simulated SLA data. Simulated Jason-1 and ENVISAT data were also obtained by sub-sampling the model fields along TOPEX/POSEIDON and ERS tracks and assuming a 2 cm rms noise for 1-second average.

The simulated data sets were then used to reconstruct the SLA gridded fields using a space-time sub-optimal interpolation method. The method is detailed in Ducet et al. (2000) and Le Traon et al. (2001). It uses the following space (zero crossing of correlation function, ZC) and time (e-folding time, ET) correlation scales :

$$ZC = 50 + 250 \left( \frac{900}{Lat^2 + 900} \right) \text{ km where Lat stands for latitude, in degrees.}$$

$$ET = 15 \text{ days}$$

These scales are intended to represent typical space and time scales of SLA as they can be observed from altimetry. The estimations are performed on a regular grid of  $1/10^\circ \times 1/10^\circ$ . For a given grid point, all the observations such as  $(d/ZC)^2 + (T/ET)^2 < 1$  are taken into account ( $d$  is the distance between the observation and the grid point and  $T$  is the time difference between the observation and grid point date). Comparison of the reconstructed fields with the reference model fields (resampled on the regular  $1/10^\circ \times 1/10^\circ$  grid) allows an estimation of the sea level and velocity mapping error. The velocity errors (and velocity reference fields) were derived from the sea level gradients (finite centered differences) through the geostrophic approximation. In practice, the comparison was made over a 6-month period (1993) with maps calculated every 9 days, i.e. we compared a total of 20 maps. The calculations were done on a large area from  $20^\circ\text{N}$  to  $60^\circ\text{N}$  and  $75^\circ\text{W}$  to  $10^\circ\text{W}$ , i.e. covering the full North Atlantic.

In addition to conventional altimeter configurations with one (Jason-1 or ENVISAT) and two satellites (Jason-1+ENVISAT), a GNSS only configuration (simulation 1) and a GNSS +Jason-1+ENVISAT configuration (simulation 2) were analyzed. Simulation 1 allows us to analyze the contribution of GNSS altimetry alone while simulation 2 allows us to analyze the complementary of GNSS altimetry with the existing and future conventional altimeter missions. It is, indeed, likely that in the coming decade the ocean will be observed at least with two conventional altimeters as it was with TOPEX/POSEIDON and ERS-1/2 and will be soon with Jason-1 and ENVISAT.

To illustrate the methodology, we show on figure 2a the LAM sea level anomaly for a given day. Figures 2b and 2c show the corresponding mapping errors for the GNSS and GNSS + Jason-1 + ENVISAT configurations. One can note that the GNSS configuration is able to capture the main energetic mesoscale signals. In low eddy energy regions, the errors are relatively larger because the measurement noise is much larger than the signal. There, the mapping errors are close to 100 % of the signal variance, i.e. no useful information is brought. Note, however, that as the noise level is taken into account in the analysis, errors are of a few cm rms only, i.e. part of the noise is filtered out in the mapping procedure (when the noise to signal ratio is very large, the estimated field will be close to zero).

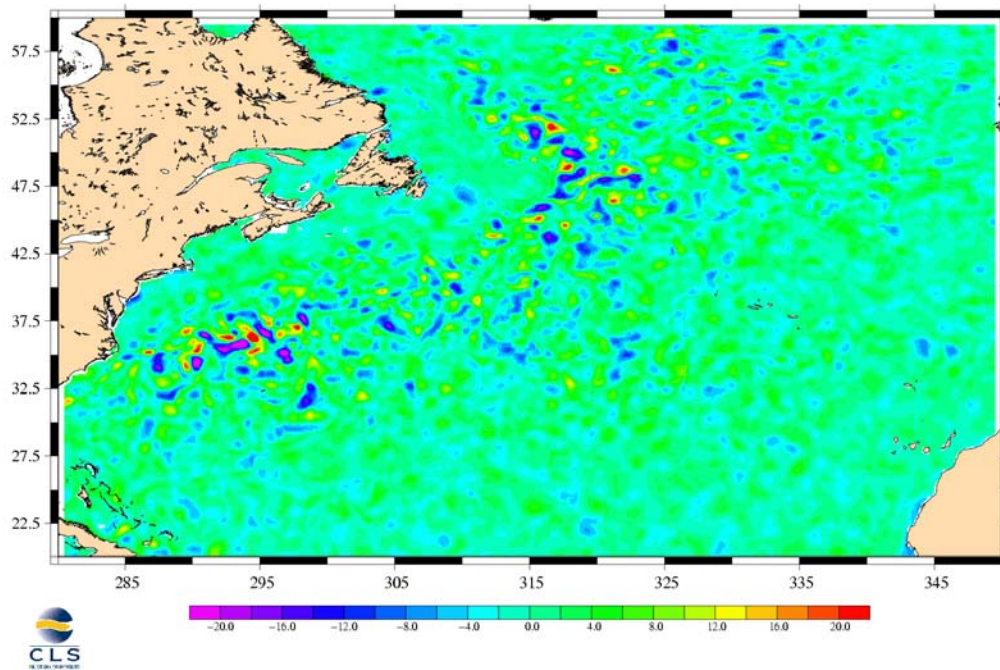
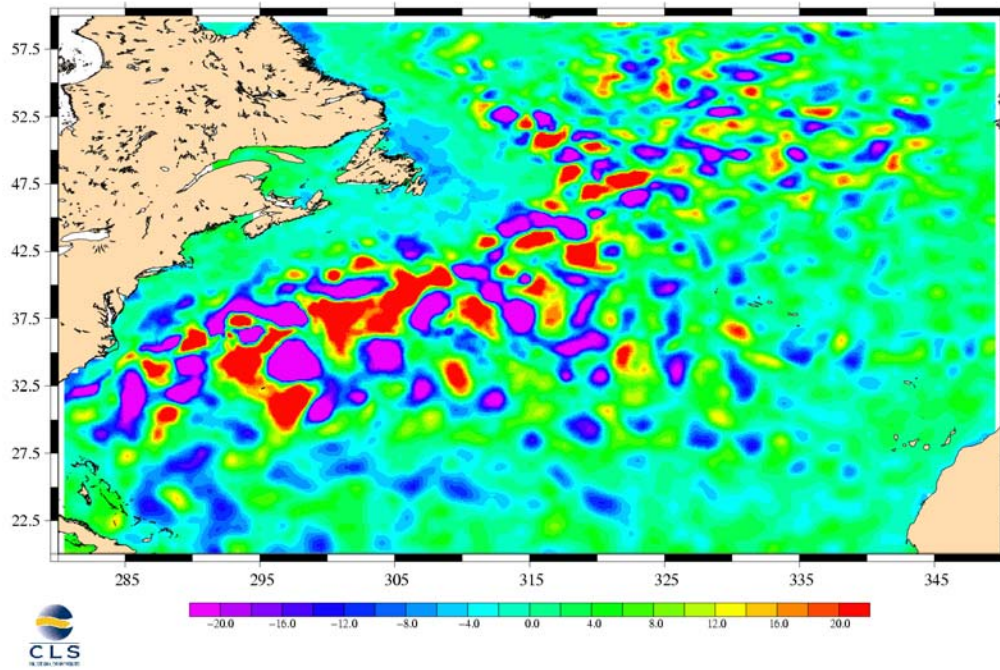


Figure 2a and 2b: Los Alamos model sea level anomaly field for a given day (a). Corresponding mapping error for the GNSS configuration (b). Units are cm.

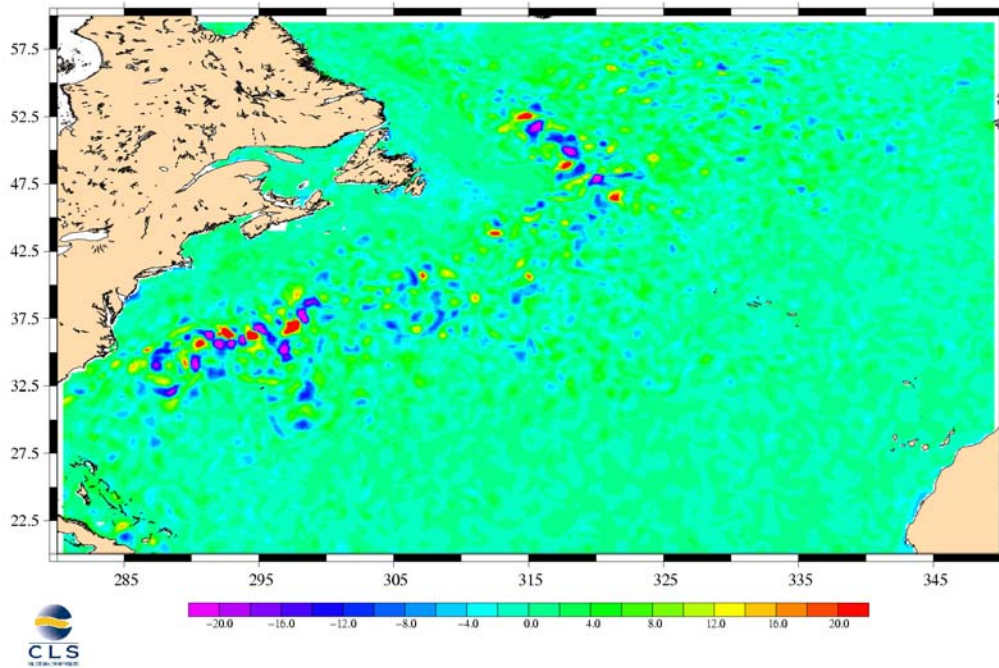


Figure 2c: Corresponding mapping error for the GNSS +Jason-1+Envisat configuration. Units are cm.

## 4 Results

As in the PARIS-beta study, the quadratic relative sea level, zonal and meridional velocity mapping errors (i.e. the ratio of the mapping error variance over the ocean signal variance) were calculated. Table 1 summarizes the results obtained for regions where the rms sea level variability is larger than 15 cm rms. This allows us to analyze the mapping capabilities for regions whose dynamics are dominated by mesoscale variability. These are the regions where we expect a significant contribution of GNSS altimetry.

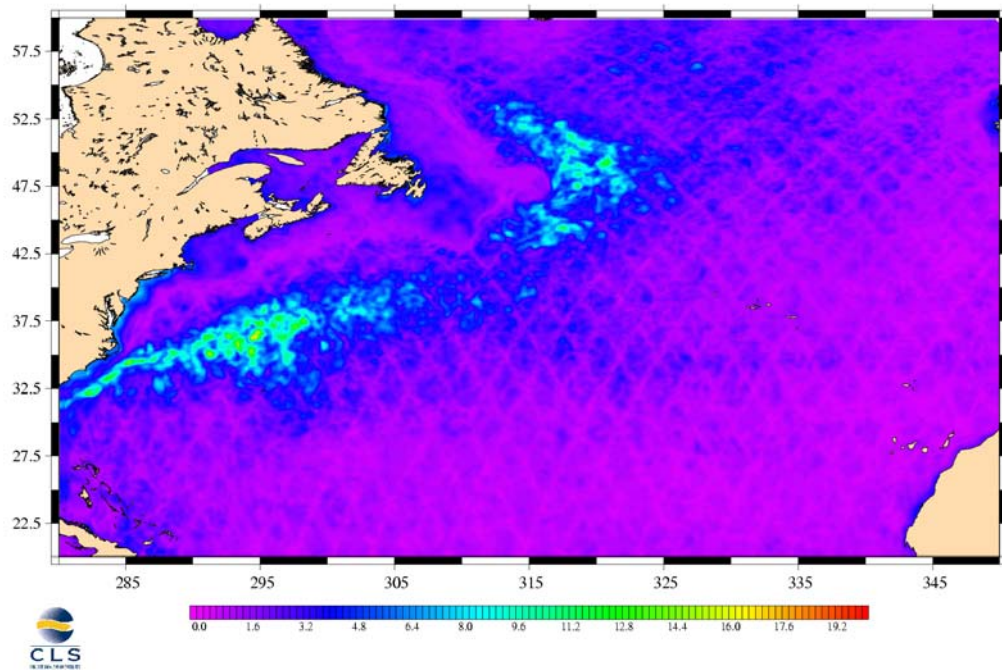
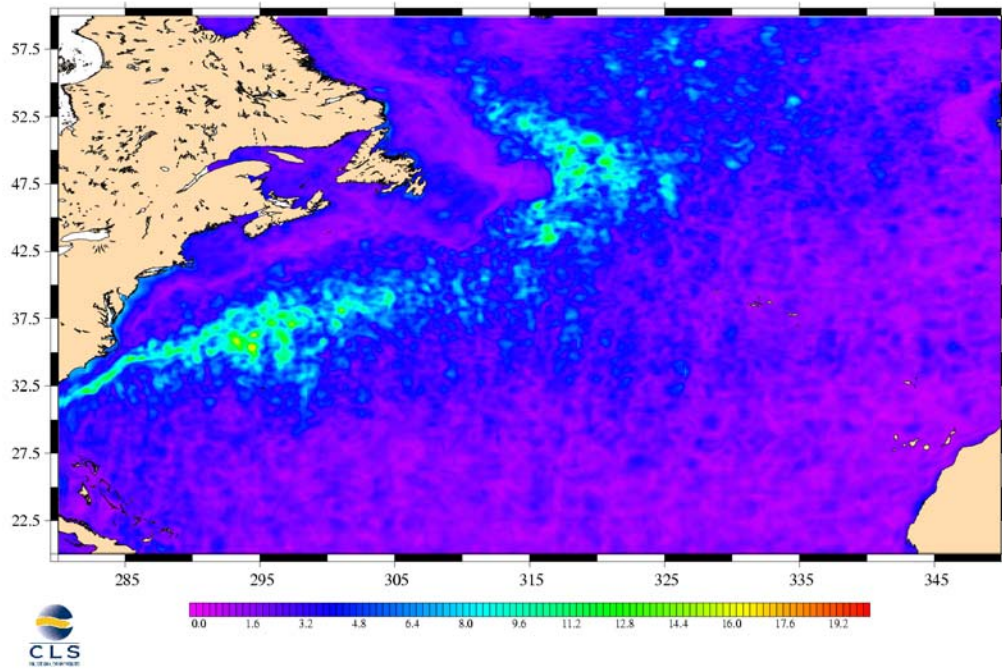
	<b>H</b>	<b>U</b>	<b>V</b>
<b>Jason-1</b>	<b>22.1</b>	<b>44.1</b>	<b>55.0</b>
<b>ENVISAT</b>	<b>12.1</b>	<b>34.5</b>	<b>45.1</b>
<b>Jason-1+ENVISAT</b>	<b>8.4</b>	<b>26.6</b>	<b>33.8</b>
<b>GNSS</b>	<b>5.7</b>	<b>26.9</b>	<b>28.5</b>
<b>GNSS +Jason-1+ENVISAT</b>	<b>4.2</b>	<b>20.2</b>	<b>24.1</b>

Table 1: Sea Level (H), zonal (U) and meridional (V) velocity mean mapping errors for regions with rms sea level variability larger than 15 cm. Errors expressed in percentage of the total sea level and velocity

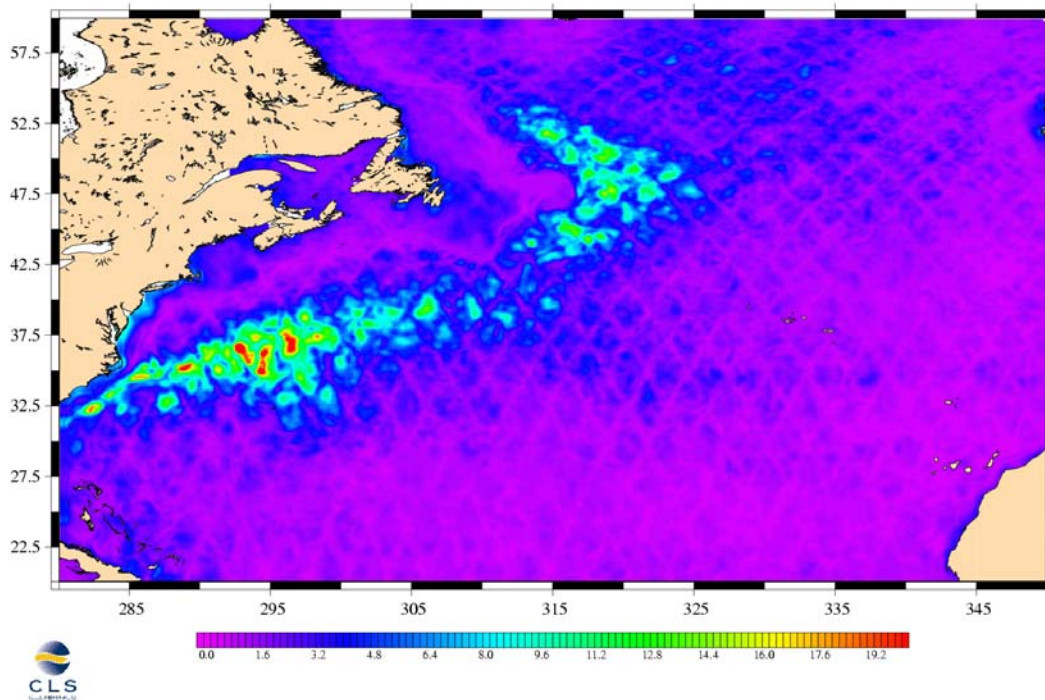
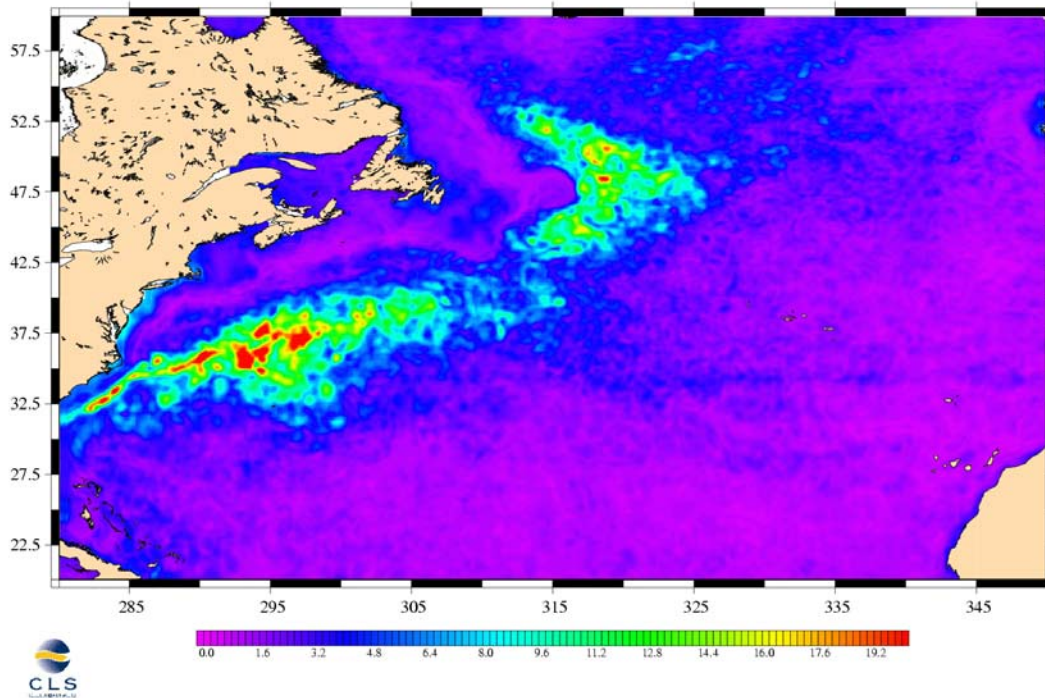
These results show that in regions with large mesoscale variability GNSS is performing better than Jason-1 + ENVISAT. The combination of GNSS with Jason-1 and ENVISAT should also improve the sea level mapping and the velocity mapping by about 30%. There is an improvement by about a factor 2 for the sea level mapping compared to the simulations performed for the PARIS-Beta study (Le Traon et al., 2002). This is mainly due of the denser sampling offered by the combination of GPS, Galileo and Inmarsat data.

In the simulated sampling we used, there are about 12 measurement points every second, i.e. 12 times more than for a conventional altimeter. The GNSS measurement noise variance is, of course, much larger than for a conventional altimeter (by a factor of up to 100) but, in high eddy variability regions, it remains smaller than the signal variance. An observation with a 10 cm rms measurement noise yields a relative mapping error of about 10% in the Gulf Stream area (where the rms sea level variability is larger than 30 cm). This is smaller than the mapping error obtained from ENVISAT and equivalent to the mapping error obtained from the combination of Jason-1 and ENVISAT.

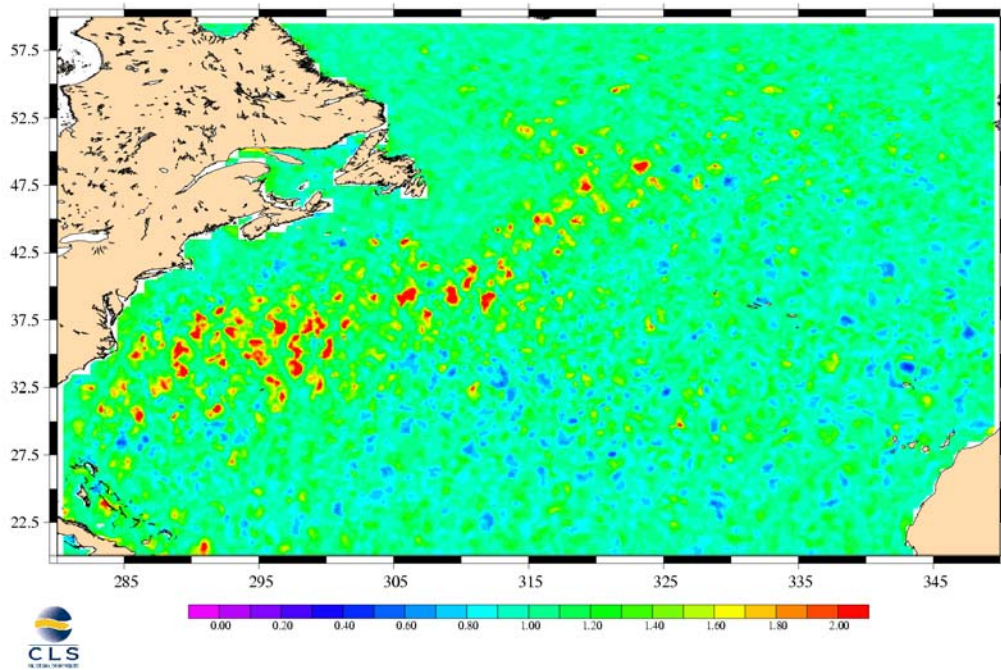
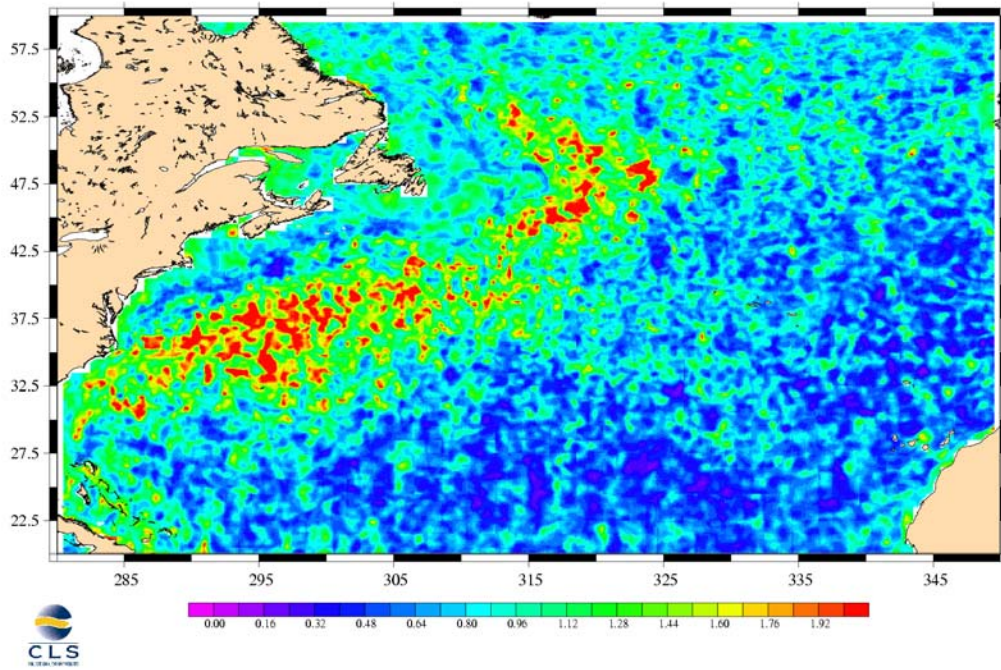
Figures 3 and 4 show the rms sea level mapping errors for simulations 1 and 2 respectively. Figure 3 is clearly related to the sampling characteristics of GNSS (see figure 1a). Errors are large when there is a poor sampling. They are also relatively large in low eddy energy regions. This is improved when GNSS data are merged with Jason-1 and ENVISAT.



Figures 3 and 4 : Rms sea level mapping error for GNSS (upper figure), GNSS +Jason-1+ ENVISAT (lower figure). Units are cm.



Figures 5 and 6 : Rms sea level mapping error for ENVISAT (upper figure) and Jason-1+ ENVISAT (lower figure). Units are cm.



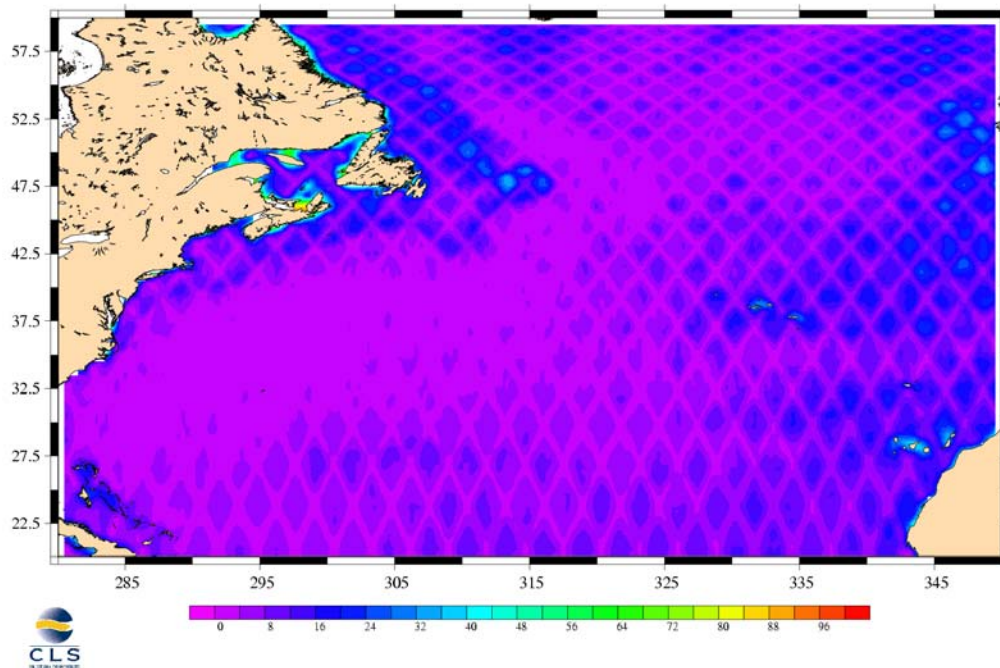
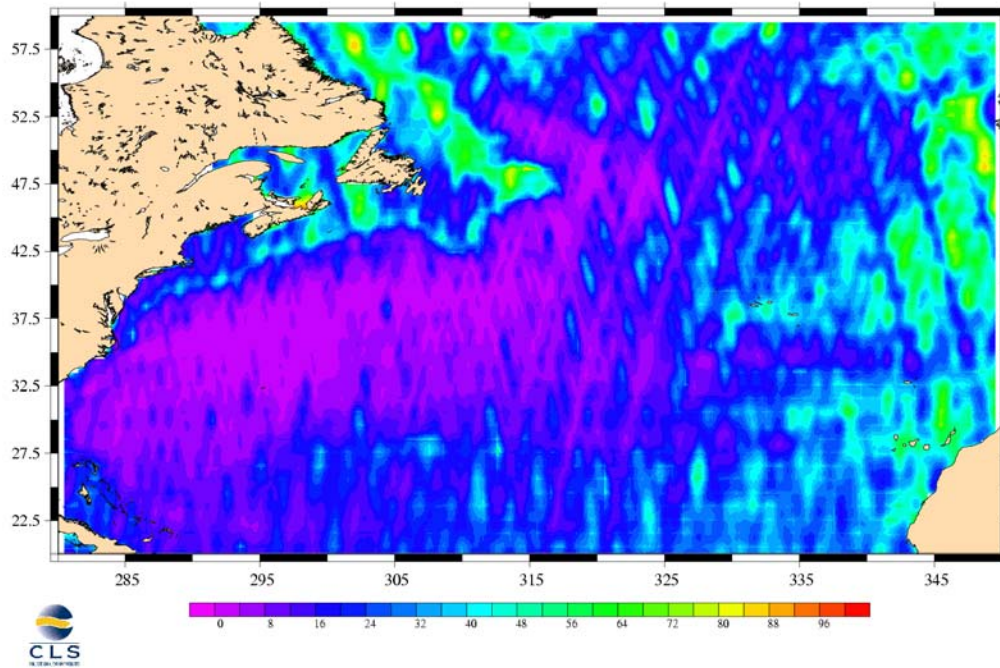
Figures 7 and 8 : rms ENVISAT sea level mapping error over rms GNSS sea level mapping error (upper figure). Rms Jason-1+ENVISAT sea level mapping error over rms GNSS + Jason-1 + ENVISAT sea level mapping error (lower figure).

Figures 3 and 4 can be compared with sea level mapping errors from one altimeter (ERS or ENVISAT) (figure 5) and from the combination of two conventional altimeters (T/P and ERS or Jason-1 and ENVISAT) (figure 6). As in table 1, these results illustrate the contribution of GNSS altimetry. In large eddy variability regions, GNSS is performing much better than Jason-1 and ENVISAT alone and better than Jason-1+ENVISAT.

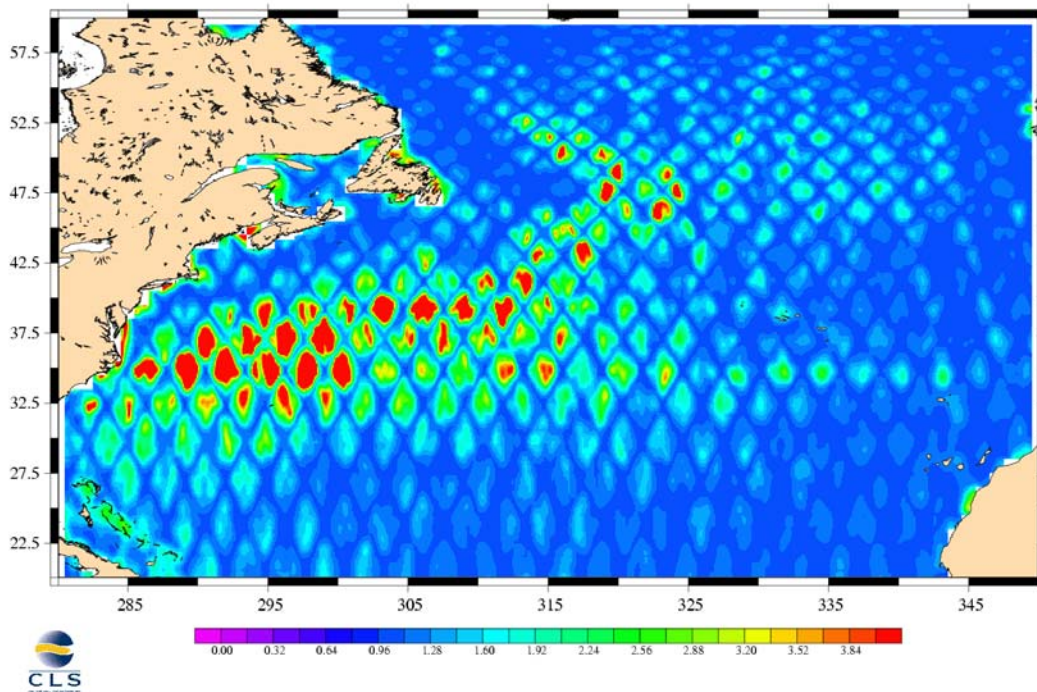
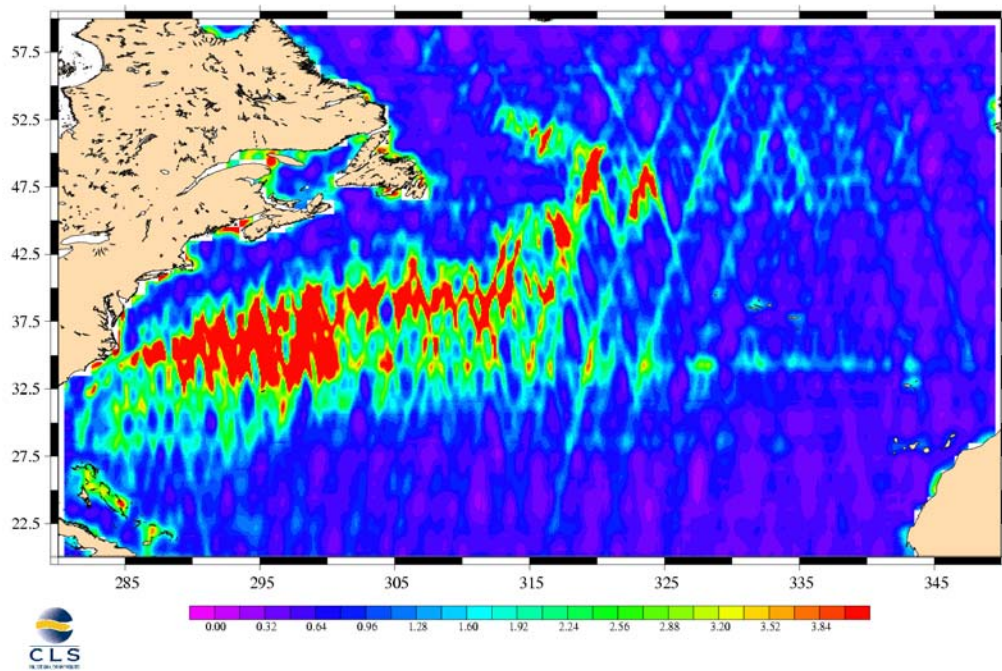
To quantify, the contribution of GNSS altimetry, the ratio between the ENVISAT and GNSS mapping error variance (figure 7) and the Jason-1+ENVISAT and GNSS +Jason-1+ENVISAT (figure 8) were also calculated. Compared to ENVISAT, in the Gulf Stream region and in well sampled regions, the GNSS mapping error variances are divided by a factor of up to 4. Compared to Jason-1+ENVISAT, the combination of GNSS, Jason-1 and ENVISAT should also allow a reduction of the mapping error variance by a factor of up to four (mainly in between the Jason-1 tracks where the mapping from the combination of Jason-1 and ENVISAT is less accurate).

## **5 Formal mapping errors**

The formal mapping errors (expressed in percentage of signal variance) were also derived from these analyses. These errors only depend on sampling, noise and signal characteristics and do not depend on model fields. They provide a robust estimation of the mapping capabilities that only depend on our choice of signal covariance functions. Figures 9 and 10 show the sea level formal mapping errors for simulations 1 and 2 respectively. The ratio between the ENVISAT and GNSS formal mapping error variance (figure 11) and the Jason-1+ENVISAT and GNSS +Jason-1+ENVISAT (figure 12) are also shown. Results are consistent with those discussed in section 4. In high eddy energy regions and well sampled regions, GNSS and GNSS +Jason-1+ENVISAT are generally performing much better than ENVISAT and Jason-1+ENVISAT respectively (mapping error variances are divided by a factor of up to 4).



Figures 9 and 10 : Formal sea level mapping error for GNSS (upper figure), and GNSS +Jason-1 + ENVISAT (lower figure). Units are percentage of signal variance.



Figures 11 and 12 : ENVISAT formal mapping error variance over GNSS formal mapping error variance (upper figure). Jason-1+ENVISAT formal mapping error variance over GNSS + Jason-1+ENVISAT formal mapping error variance (lower figure).

## 6 Conclusions

A PETREL-like mission (with a multibeam upgrade – up to 12 signals from GPS, Galileo and Inmarsat satellites) should thus have a very significant impact on the mapping of the mesoscale variability. According to the chosen error budget, it should allow us to map the mesoscale variability in high eddy variability regions better than Jason-1+ENVISAT.

Moreover, the combination of GNSS with Jason-1 and ENVISAT will improve the sea level mapping derived from the combination of Jason-1 and ENVISAT by a factor of about 2. In well sampled regions, the improvement could reach up to a factor of 4.

Although there are other sources of errors that should be taken into account (e.g. propagation effects, orbit, geoid), this is a very encouraging result. The dense and high frequency sampling offered by multibeam GNSS altimetry is thus likely to compensate for the large noise level (20 to 30 cm for 3 second-average) (in large eddy variability regions).

Results presented in this report show an improvement by a factor of about 2 compared to the PARIS-Beta study although the error budget for this study is higher. This is mainly due to the use of both GPS and Galileo signals (up to 12 reflected signals for only 5 in PARIS-Beta).

For a future study, as already recommended in the PARIS-Beta study, the priority should be to take into account the error spectrum (when known) (i.e correlation of errors) and to redo the simulations described in this report taking into account this refined error budget.

## 7 References

Ducet, N., P.-Y. Le Traon, and G. Reverdin, 2000: Global high resolution mapping of ocean circulation from TOPEX/Poseidon and ERS-1/2. *J. Geophys. Res.*, 105, 19477-19498.

Le Traon, P.-Y. and G. Dibarboure, 1999: Mesoscale mapping capabilities of multiple-satellite altimeter missions. *J. Atmos. Oceanic Technol.*, 16, 1208-1223.

Le Traon, P.-Y., G. Dibarboure, and N. Ducet, 2001: Use of a High-Resolution Model to Analyze the Mapping Capabilities of Multiple-Altitude Missions. *J. Atmos. Oceanic Technol.*, 18, 1277-1288.

Le Traon, P.Y., G. Dibarboure, G. Ruffini, E. Cardellach, Mesoscale Ocean Altimetry Requirements and Impact of GPS-R measurements for Ocean Mesoscale Circulation Mapping, Abridged Starlab ESA/ESTEC Technical Report from the Paris Beta project, ESA/ESTEC Contract 15083/01/NL/MM, Courtesy of ESA/ESTEC and Starlab, <http://arxiv.org/abs/physics/0212068>, Dec 2002.